Unscented Kalman filter for real-time vehicle lateral tire forces and sideslip angle estimation

Moustapha Doumiati, Alessandro Victorino, Ali Charara and Daniel Lechner

***Abstract*— Knowledge of vehicle dynamic parameters is important for vehicle control systems that aim to enhance vehicle handling and passenger safety. Unfortunately, some fundamental parameters like tire-road forces and sideslip angle are difficult to measure in a car, for both technical and economic reasons. Therefore, this study presents a dynamic modeling and observation method to estimate these variables. The ability to accurately estimate lateral tire forces and sideslip angle is a critical determinant in the performances of many vehicle control system and making vehicle's danger indices. To address system nonlinearities and unmodeled dynamics, an observer derived from unscented Kalman filtering technique is proposed. The estimation process method is based on the dynamic response of a vehicle instrumented with easily-available standard sensors. Performances are tested using an experimental car in real driving situations. Experimental results show the potentiel of the estimation method.**

I. INTRODUCTION

Today, automotive electronic technologies are developing for safe and comfortable travelling of drivers and passengers. There are a lot of vehicle control system such as Rollover Prevention System, Adaptive Cruise Control System, Electronic Stability Control (ESC) and so on. These control systems installation rate is increasing all around the world.
Vehicle control algorithms have made great strides towards improving the handling and safety of vehicles. For example, experts estimate that ESC prevents 27% of loss-of-control accidents by intervening when emergency situations are detected [1]. While nowadays vehicle control algorithms are undoubtedly a life-saving technology, they are limited by the available vehicle state information.
Vehicle control systems currently available on production cars rely on available inexpensive measurements such as longitudinal velocity, accelerations and yaw rate. Sideslip rate can be evaluated using yaw rate, lateral acceleration and vehicle velocity [2]. However, calculating sideslip angle from sideslip rate integration is prone to uncertainty and errors from sensor bias. Besides, these control systems use unsophisticated, inaccurate tire models to evaluate lateral tire dynamics. In fact, measuring tire forces and sideslip angles is very difficult for technical, physical and economic reasons. Therefore, these important data must be observed or estimated. If control systems were in possession of the complete set of lateral tire characteristics, namely lateral forces, sideslip angle and the tire-road friction coefficient, they could greatly enhance vehicle handling and increase passenger safety.
As the motion of a vehicle is governed by the forces generated between the tires and the road, knowledge of the tire forces is crucial when predicting vehicle motion. Accurate data about tire forces and sideslip angle leads to a better evaluation of road friction and the vehicles possible trajectories, and to better vehicle control. Moreover, it makes possible the development of a diagnostic tool for evaluating the potential risks of accidents related to poor adherence or dangerous maneuvers.
Vehicle dynamic estimation has been widely discussed in the literature. Several studies have been conducted regarding the estimation of tire-road forces, sideslip angle and the friction coefficient. For example, in [9], the authors estimate longitudinal and lateral vehicle velocities and evaluate sideslip angle and lateral forces. In [13] and [5], sideslip angle estimation is discussed in detail. More recently, the sum of front and rear lateral forces have been estimated in [4] and [6]. However, lateral forces at each tire/road level were not estimated. Other studies present valid tire/road force observers, but these involve wheel-torque measurements requiring expensive sensors [15].
The goal of this study is to develop an estimation method that uses a simple vehicle model and a certain number of valid measurements in order to estimate in real-time the lateral force at each tire-road contact point and the sideslip angle. The observation system is highly nonlinear and presents unmodeled dynamics. For this reason, an observer based on UKF (the Unscented Kalman Filter) is proposed.
In order to show the effectiveness of the estimation method, some validation tests were carried out on an instrumented vehicle in realistic driving situations.
The remainder of the paper is organized as follows. Section 2 describes briefly the estimation process algorithm. Section 3 presents and discusses the vehicle model and the tire-road interaction phenomenon. Section 4 describes the observer and presents the observability analysis. In section 5 the results are discussed and compared to real experimental data, and then in the final section we make some concluding remarks regarding our study and future perspectives.

II. ESTIMATION PROCESS DESCRIPTION

The estimation process is shown in its entirety by the block diagram in figure 1, where a_x and a_{ym} are respectively the longitudinal and lateral accelerations, $\dot{\psi}$ is the yaw rate, $\dot{\theta}$ is the roll rate, Δ_{ij} (i represents the front(1) or the rear(2) and j represents the left(1) or the right (2)) is the suspension deflection, w_{ij} is the wheel velocity, F_{zij} and F_{yij} are respectively the normal and lateral tire-road forces, β is the sideslip angle at the center of gravity (cog). The estimation process consists of two blocks, and its role is to estimate sideslip angle, normal and lateral forces at each tire/road contact point, and consequently evaluate the used lateral friction coefficient. The following measurements are needed:

- yaw and roll rates measured by gyrometers,
- longitudinal and lateral accelerations measured by accelerometers,
- suspension deflections using suspension deflections sensors,
- steering angle measured by an optical sensor,
- rotational velocity for each wheel given by magnetic sensors.

M. Doumiati, A. Victorino and A. Charara are with Heudiasyc Laboratory, UMR CNRS 6599, Université de Technologie de Compiègne, 60205 Compiègne, France mdoumiat@hds.utc.fr, acorreav@hds.utc.fr and acharara@hds.utc.fr

D. Lechner is with Inrets-MA Laboratory, Departement of Accident Mechanism Analysis, Chemin de la Croix Blanche, 13300 Salon de Provence, France daniel.lechner@inrets.fr

978-1-4244-3504-3/09/$25.00 ©2009 IEEE

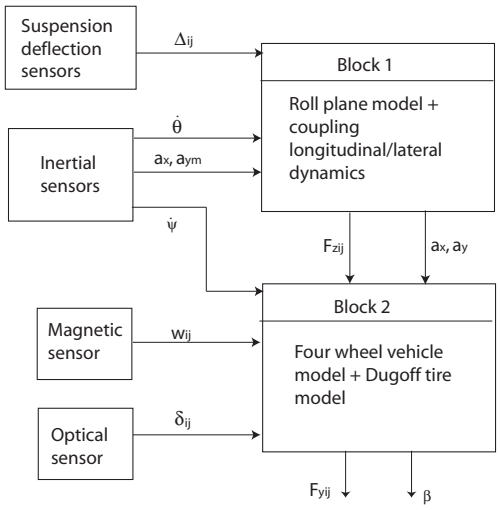

Fig. 1. Process estimation diagram

The first block aims to provide the vehicle's weight, lateral load transfer, normal tire forces and the corrected lateral acceleration a_y (by canceling the gravitational acceleration component that distorts the accelerometer signal a_{ym}). We have looked in detail at the first block in a previous study [11]. This article focuses only on the second block, whose main role is to estimate lateral tire forces and sideslip angle. The second block makes use of the estimations provided by the first block. In fact, it is of major importance to include the impact of accurate normal forces in the calculation of lateral forces.
One specificity of this estimation process is the use of blocks in series. By using cascaded observers, the observability problems entailed by an inappropriate use of the complete modeling equations are avoided, enabling the estimation process to be carried out in a simple and practical way.

III. Vehicle-road model

This section presents the vehicle model and tire-road interaction dynamics, especially the lateral tire forces. Since the quality of the observer largely depends on the accuracy of the vehicle and tire models, the underlying models must be precise. Taking real-time calculation requirement, the models should also be simple.

A. Four-wheel vehicle model

The Four-Wheel Vehicle model (FWVM) is chosen for this study because it is simple and corresponds sufficiently to our objectives. The FWVM is widely used to describe transversal vehicle dynamic behavior [4], [9], [5].
Figure 2 shows a simple diagram of the FWVM model in the longitudinal-lateral plane. In order to simplify the lateral and longitudinal dynamics, drive force and rolling resistance were neglected. Additionally, the front and rear track widths (E) are assumed to be equal. L_1 and L_2 represent the distance from the vehicle's center of gravity to the front and rear axles respectively. The sideslip at the vehicle center of gravity (β) is the difference between the velocity heading (V_g) and the true heading of the vehicle (ψ). The yaw rate ($\dot{\psi}$) is the angular velocity of the vehicle about the center of gravity. The longitudinal and lateral forces ($F_{x,y,i,j}$) are shown for front and rear tires of the vehicle. Assuming front-wheel drive, rear longitudinal forces are neglected relative to the front longitudinal forces; we assume that $F_{x1} = F_{x11} + F_{x12}$.
The lateral dynamics of the vehicle can be obtained by summing the forces and moments about the vehicle's center of gravity. Consequently, the simplified FWVM is formulated as the following dynamic relationship:

$$\begin{aligned}
\dot{V_g} &= \tfrac{1}{m}\begin{bmatrix} F_{x1}\cos(\beta-\delta) + F_{y11}\sin(\beta-\delta) + \\ F_{y12}\sin(\beta-\delta) + (F_{y21}+F_{y22})\sin\beta \end{bmatrix},\\
\ddot{\psi} &= \tfrac{1}{I_z}\begin{bmatrix} L_1[F_{y11}\cos\delta + F_{y12}\cos\delta + F_{x1}\sin\delta] - \\ L_2[F_{y21}+F_{y22}] + \\ \frac{E}{2}[F_{y11}\sin\delta - F_{y12}\sin\delta] \end{bmatrix},\\
\dot{\beta} &= \tfrac{1}{mV_g}\begin{bmatrix} -F_{x1}\sin(\beta-\delta) + F_{y11}\cos(\beta-\delta) + \\ F_{y12}\cos(\beta-\delta) + (F_{y21}+F_{y22})\cos\beta \end{bmatrix} - \dot{\psi},\\
a_y &= \tfrac{1}{m}[F_{y11}\cos\delta + F_{y12}\cos\delta + (F_{y21}+F_{y22}) + F_{x1}sin\delta],\\
a_x &= \tfrac{1}{m}[-F_{y11}\sin\delta - F_{y12}\sin\delta + F_{x1}\cos\delta],
\end{aligned} \tag{1}$$

where m is the vehicle mass, and I_z the yaw moment of inertia.
The tire slip angle (α_{ij}), as shown in figure 2, is the difference between the tire's longitudinal axis and the tire's velocity vector. The tire velocity vector can be obtained from the vehicle's velocity (at the cog) and the yaw rate. Assuming that rear steering angles are approximately null, the direction or heading of the rear tires is the same as that of the vehicle. The heading of the front tires includes the steering angle (δ). The front steering angles are assumed to be equal ($\delta_{11} = \delta_{12} = \delta$). The vehicle velocity V_g, steering angle δ, yaw rate $\dot{\psi}$ and the vehicle body slip angle β are then used to calculate the tire slip angles α_{ij}, where:

$$\begin{aligned}
\alpha_{11} &= \delta - \arctan\left[\tfrac{V_g\beta + L_1\dot{\psi}}{V_g - E\dot{\psi}/2}\right],\\
\alpha_{12} &= \delta - \arctan\left[\tfrac{V_g\beta + L_1\dot{\psi}}{V_g + E\dot{\psi}/2}\right],\\
\alpha_{21} &= -\arctan\left[\tfrac{V_g\beta - L_2\dot{\psi}}{V_g - E\dot{\psi}/2}\right],\\
\alpha_{22} &= -\arctan\left[\tfrac{V_g\beta - L_2\dot{\psi}}{V_g + E\dot{\psi}/2}\right].
\end{aligned} \tag{2}$$

B. lateral tire-force model

The model of tire-road contact forces is complex because a wide variety of parameters including environmental factors and pneumatic properties (load, tire pressure, etc.) impact the tire-road contact interface. Many different tire models are to be found in the literature, based on the physical nature of the tire and/or on empirical formulations deriving from experimental data, such as the Pacejka, Dugoff and Burckhardt models [8], [7], [5]. Dugoff's model was selected for this study because of the small number of parameters that are sufficient to evaluate the tire-road forces. The nonlinear lateral tire forces are given by:

$$F_{yij} = -C_{\alpha i} tan\alpha_{ij}.f(\lambda) \tag{3}$$

where $C_{\alpha i}$ is the lateral stiffness, α_{ij} is the slip angle and $f(\lambda)$ is given by:

$$f(\lambda) = \begin{cases} (2-\lambda)\lambda, & \text{if } \lambda < 1 \\ 1, & \text{if } \lambda \geq 1 \end{cases} \tag{4}$$

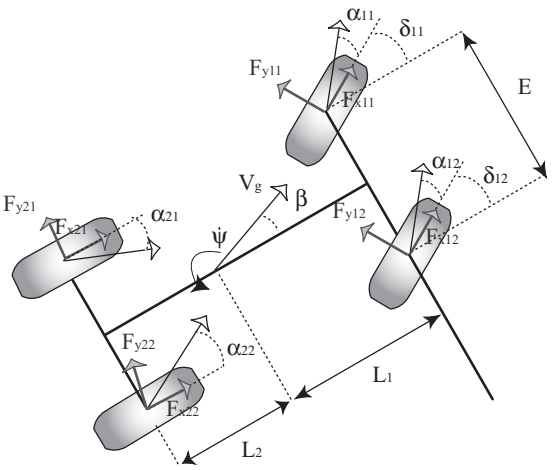

Fig. 2. Four-wheel vehicle model.

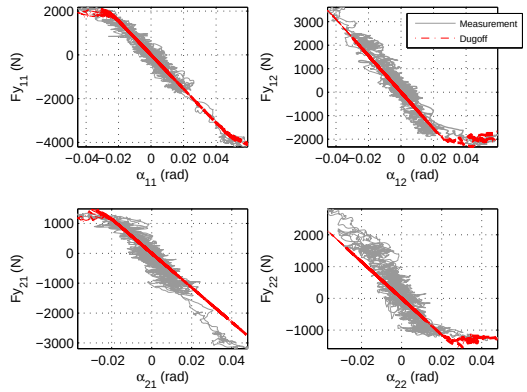

Fig. 3. Validation of the Dugoff model.

$$\lambda = \frac{\mu F_{zij}}{2C_{\alpha_i}\,|tan\alpha_{ij}|} \tag{5}$$

In the above formulation, μ is the coefficient of friction of the road and F_{zij} is the normal load on the tire. This simplified tire model assumes no longitudinal forces, a uniform pressure distribution, a rigid tire carcass, and a constant coefficient of friction of sliding rubber.
In order to validate the chosen model, many tests were carried out using a laboratory car (see section V-A). Figure 3 compares measured forces and the Dugoff model. These results prove the model validity.
As shown in figure 3, the relationship between the lateral force and the slip angle is initially linear (low slip angles). When operating in the linear region, a vehicle responds predictably to the driver's inputs. As the vehicle approaches the handling limits, for example during an evasive emergency maneuver, or when a vehicle undergoes high accelerations, high slip angles occur and the vehicle's dynamic becomes highly nonlinear and its response becomes less predictable and potentially very dangerous.

C. Relaxation model

When vehicle sideslip angle changes, a lateral tire force is created with a time lag. This transient behavior of tires can be formulated using a relaxation length σ. The relaxation length is the distance covered by the tire while the tire force is kicking in. Using the relaxation model presented in [3], lateral forces can be written as:

$$\dot{F}_{yij} = \frac{V_g}{\sigma_i}(-F_{yij} + \overline{F_{yij}}), \tag{6}$$

where $\overline{Fy_{ij}}$ is calculated from a Dugoff tire-force model, V_g is the vehicle velocity and σ_i is the relaxation length.

IV. Observers Design

This section presents a description of the observer devoted to lateral tire forces and sideslip angle. The state-space formulation, the observability analysis and the estimation method will be presented.

A. Stochastic state-space representation

The nonlinear stochastic state-space representation of the system described in previous section is given as:

$$\begin{cases} \dot{X}(t) &= f(X(t),U(t)) + w(t) \\ Y(t) &= h(X(t),U(t)) + v(t) \end{cases} \tag{7}$$

The input vector U comprises the steering angle and the normal forces considered estimated by the first block (see figure 1):

$$U = [\delta,\ F_{z11},\ F_{z12},,\ F_{z21},\ F_{z22}]. \tag{8}$$

The measure vector Y(t) comprises yaw rate, vehicle velocity (approximated by the mean of the rear wheel velocities calculated from wheel-encoder data), longitudinal and lateral accelerations:

$$Y = [\dot{\psi},\ V_g,\ a_x,\ a_y]. \tag{9}$$

The state vector comprises yaw rate, vehicle velocity, sideslip angle at the cog, lateral forces and the sum of the front longitudinal tire forces:

$$X = [\dot{\psi},\ V_g,\ \beta,\ F_{y11},\ F_{y12},\ F_{y21},\ F_{y22},\ F_{x1}]. \tag{10}$$

The process and measurements noise vectors, respectively $w(t)$ and $v(t)$, are assumed to be white, zero mean and uncorrelated.
The nonlinear functions (f) and (h) representing the state and the observation equations are calculated according to equations (1) and (6).

B. Observability

Observability is a measure of how well the internal states of a system can be inferred from knowledge of its inputs and external outputs. This property is often presented as a rank condition on the observability matrix. Using the nonlinear state-space formulation of the system presented in section IV-A, the observability definition is local and uses the Lie derivative [12]. An observability analysis of this system was undertaken in [14]. It was shown that the system is observable except when:

- steering angles are null,
- the vehicle is at rest ($V_g = 0$).

For these situations, we assume that lateral forces and sideslip angle are null, which approximately corresponds to the real cases.

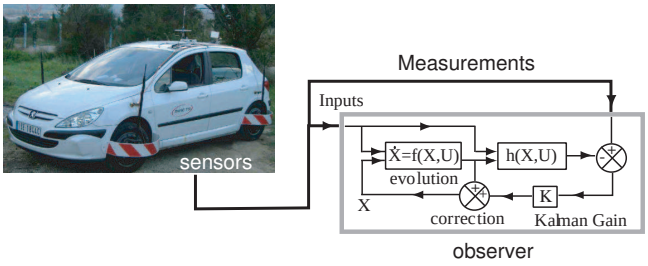

Fig. 4. Process estimation diagram

C. Estimation method

The aim of an observer or a virtual sensor is to estimate a particular unmeasurable variable from available measurements and a system model in a closed loop observation scheme, as illustrated in figure 4. The observer was implemented in a first-order Euler approximation discrete form. At each iteration, the state vector is first calculated according to the evolution equation and then corrected online with the measurement errors and the filter gain K in a recursive prediction-correction mechanism. The gain is calculated using the Kalman filter technique (EKF, UKF, ...). The EKF (Extended Kalman Filter) is probably the most commonly-used estimator for nonlinear systems. However, in this study the UKF (Unscented Kalman Filter) [16] is chosen for the following reasons:

- the high nonlinearities of the vehicle-road model,
- the calculation complexity of the Jacobian matrices which causes implementation difficulties.

1) UKF algorithm: In this subsection, the principle of the UKF is summarized. Consider the general discrete nonlinear system:

$$\begin{cases} X_{k+1} &= f(X_k, U_k) + w_k \\ Y_k &= h(X_k) + v_k \end{cases} \tag{11}$$

where $X_k \in R^n$ is the state vector, $U_k \in R^r$ is the known input vector, $Y_k \in R^m$ is the output vector at time k. w_k and v_k are, respectively, the disturbance and sensor noise vector, which are assumed to be Gaussian white noise with zero mean and uncorrelated.
The UKF can be formulated as follows:
Initialization

$$\begin{cases} \bar{X}_0 &= E[X_0] \\ P_0 &= E[(X_0 - \bar{X}_0)(X_0 - \bar{X}_0)^T] \end{cases} \tag{12}$$

where $\bar{X}_0$ and P_0 are respectively the initial state and the initial covariance.
Sigma points calculation and time update

$$\begin{cases} \chi_{k-1} &= [\bar{X}_{k-1}, \bar{X}_{k-1} \pm \sqrt{(n+\lambda)P_{k-1}}] \\ \chi^*_{k|k-1} &= f(\chi_{k-1}, U_{k-1}) \\ \bar{x}_{k|k-1} &= \sum_{i=0}^{2n} w_i^m \chi^*_{i,k|k-1} \\ P_{k|k-1} &= \sum_{i=0}^{2n} w_i^c (\chi^*_{i,k|k-1} - \bar{X}_{k|k-1}) \times \\ & \quad (\gamma^*_{i,k|k-1} - \bar{X}_{k|k-1})^T + Q \\ \chi_{k|k-1} &= [\bar{X}_{k-1}, \bar{X}_{k-1} \pm \sqrt{(n+\lambda)P_{k|k-1}}] \\ \gamma_{k|k-1} &= h(\chi_{k|k-1}) \\ \bar{Y}_{k|k-1} &= \sum_{i=0}^{2n} w_i^m \gamma_{i,k|k-1} \end{cases} \tag{13}$$

where

$$\begin{cases} w_0^m &= \frac{\lambda}{n+\lambda} \\ w_0^c &= \frac{\lambda}{n+\lambda} + (n - \alpha^2 + \beta) \\ w_i^m &= w_i^c = \frac{1}{2(n+\lambda)} \quad i = 1, \ldots, 2n \\ \lambda &= n(\alpha^2 - 1) \end{cases} \tag{14}$$

Measurement update

$$\begin{cases} P_{\bar{Y}_k \bar{Y}_k} &= \sum_{i=0}^{2n} w_i^c (\gamma_{i,k|k-1} - \bar{Y}_{k|k-1}) \times \\ & \quad (\gamma_{i,k|k-1} - \bar{Y}_{k|k-1})^T + R \\ P_{\bar{X}_k \bar{Y}_k} &= \sum_{i=0}^{2n} w_i^c (\chi_{i,k|k-1} - \bar{X}_{k|k-1}) \times \\ & \quad (\gamma_{i,k|k-1} - \bar{Y}_{k|k-1})^T \\ K_k &= P_{\bar{X}_k \bar{Y}_k} P^{-1}_{\bar{Y}_k \bar{Y}_k} \\ P_k &= P_{k|k-1} - K_k P_{\bar{Y}_k \bar{Y}_k} K_k^T \\ \bar{X}_k &= \bar{X}_{k|k-1} + K_k (Y_k - \bar{Y}_{k|k-1}) \end{cases} \tag{15}$$

where the variables are defined as follows: $\bar{X}_k$ and $\bar{Y}_{k|k-1}$ are the estimations respectively of the state and of the real measurement at each instant k. w_i is a set of scalar weights, and n is the state dimension; the parameter α determines the spread of the sigma points around $\bar{X}$ and is usually set to $1e-4 < \alpha < 1$. The constant β is used to incorporate part of the prior knowledge of the distribution of X, and for Gaussian distributions, $\beta = 2$ is optimal. Q and R are respectively the disturbance and sensor-noise covariance: R takes into account the uncertainty in the measured data and Q is tuned depending on the model quality.

V. Experimental results

In this section we present the experimental car used to test the observers potential, and we discuss and analyze the test conditions and the observers' results.

A. Experimental car

The experimental vehicle shown in figure 4 is the INRETS-MA (Institut National de la Recherche sur les Transports et leur Sécurité - Département Mécanismes d'Accidents) Laboratory's test vehicle [2]. It is a Peugeot 307 equipped with a number of sensors including accelerometers, gyrometers, steering angle sensors, linear relative suspension sensors, three Correvits and four dynamometric wheels. One Correvit is located in chassis rear overhanging position and it measures longitudinal and lateral vehicle speeds and two Correvits are installed on the front right and rear right tires and they measure front and rear tires velocities and sideslip angles. The dynamometric wheels fitted on all four tires, which are able to measure tire forces and wheel torques in and around all three dimensions.
We note that the correvit and the wheel-force transducer (see figure 5) are very expensive sensors. The sampling frequency of the different sensors is 100 Hz.

B. Test conditions

Test data from nominal as well as adverse driving conditions were used to assess the performance of the observer presented in section IV, in realistic driving situations. We report a lane-change manoeuvre where the dynamic contributions play an important role. Figure 6 presents the Peugeot's trajectory (on a dry road), its speed, steering angle and "g-g" acceleration diagram during the course of the test. The acceleration diagram, that determines the maneuvering area utilized by the driver/vehicle, shows that large lateral accelerations were obtained (absolute value up to $0.6g$). This means that the experimental vehicle was put in a critical driving situation.

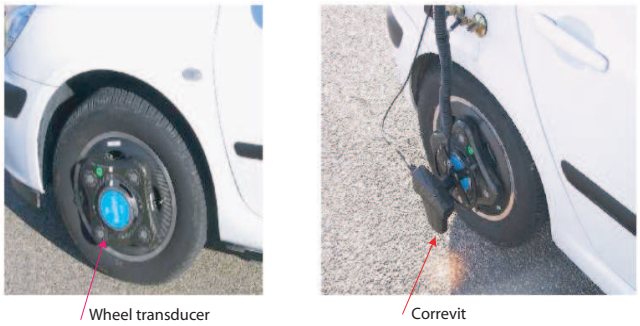

Fig. 5. Wheel-force transducer and sideslip sensor installed at the tire level.

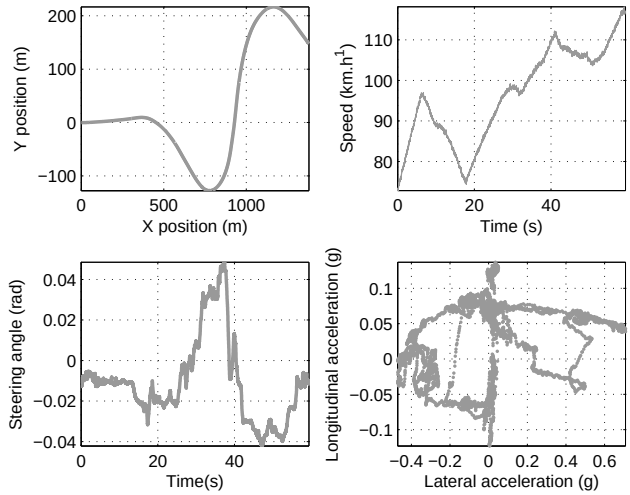

Fig. 6. Experimental test: vehicle trajectory, speed, steering angle and acceleration diagrams for the lane-change test

The estimation process algorithm was written in C++ and has been integrated into the laboratory car as a DLL (Dynamic Link Library) that functions according to the software acquisition system.

C. Validation of observers

The observer results are presented in two forms: as tables of normalized errors, and as figures comparing the measurements and the estimations. The normalized error for an estimation z is defined as:

$$\epsilon_z = 100 \times \frac{\|z_{obs} - z_{measured}\|}{max(\|z_{measured}\|)} \quad (16)$$

where z_{obs} is the variable calculated by the observer, $z_{measured}$ is the measured variable and $max(\|z_{measured}\|)$ is the absolute maximum value of the measured variable during the test maneuver.

Figures 7 and 8 show lateral forces on the front and rear wheels. According to these plots, the observers are relatively good with respect to measurements. Some small differences during the trajectory are to be noted. These might be explained by neglected geometrical parameters, especially the camber angles, which also produce a lateral forces component [10]. It is also shown that the lateral forces on the right-hand tires exceed those on the left-hand tires.

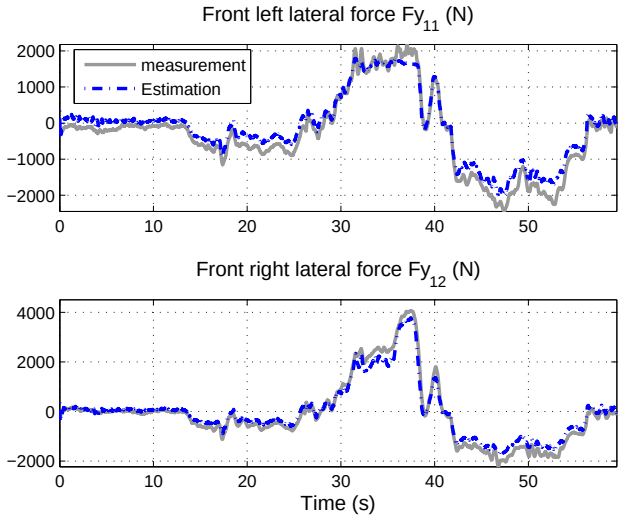

Fig. 7. Estimation of front lateral tire forces.

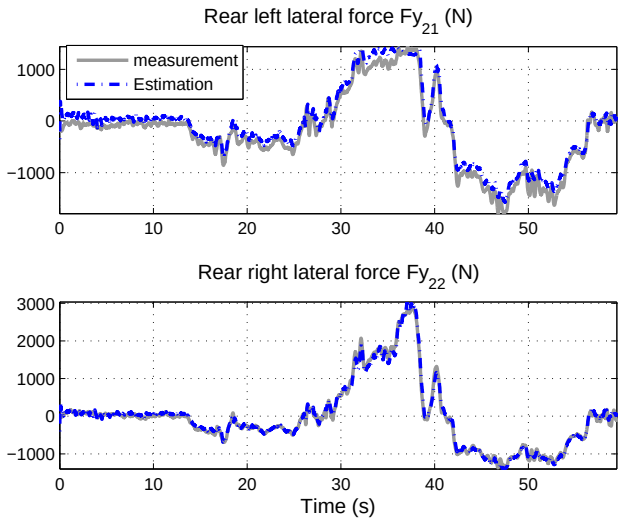

Fig. 8. Estimation of rear lateral tire forces.

This result is clearly a consequence of the load transfer produced during cornering from the left to the right-hand side of the vehicle. In fact, lateral force increases as normal force increases. Figure 9 shows how sideslip angle changes during the test. Reported results are relatively good.

Table I presents maximum absolute values, normalized mean errors and normalized std (standard deviations) for lateral tire forces and sideslip angles. Despite the simplicity of the model, we can deduce that for this test, the performance of the observer is satisfactory, with normalized error globally less than 8%.

Given the vertical and lateral tire forces at each tire-road contact level, the estimation process is able to evaluate the used lateral friction coefficient μ. This is defined as the ratio of friction force to normal force, and is given by [10]:

$$\mu_{ij} = \frac{Fy_{ij}}{Fz_{ij}} \quad (17)$$

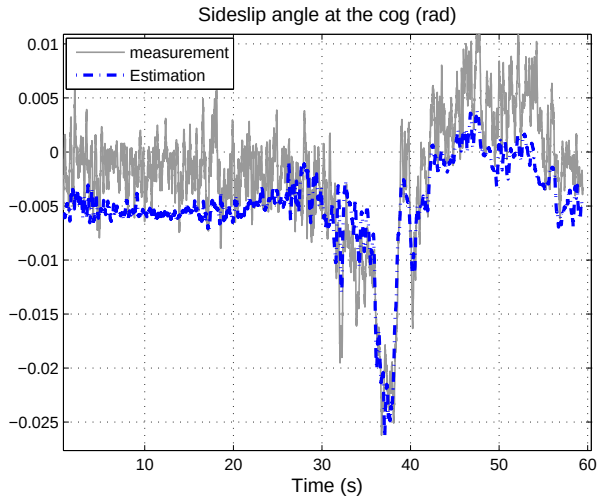

Fig. 9. Estimation of the sideslip angle at the cog.

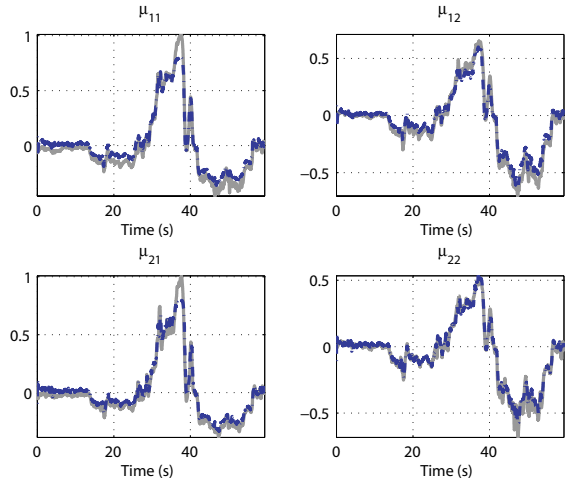

Fig. 10. Used lateral friction coefficients developed by the tires

The lateral friction coefficients in figure 10 show that the estimated μ_{ij} are close to the measured values. A closer investigation reveals that the used lateral friction coefficients μ_{12} and μ_{22} corresponding to the overloaded tires during cornering are lower than μ_{11} and μ_{21}. This phenomenon is due to the tire load sensitivity effect: the lateral friction coefficient is normally higher for the lighter loads, or conversely, falls off as the load increases [10].
This test also demonstrates that μ_{11} and μ_{21} are high, especially for lateral accelerations up to 0.6, and that they attain the limit for the dry road friction coefficient. In fact, dry road surfaces show a high friction coefficient in the range 0.9-1.2 (implying that driving on these surfaces is safe), which means that for this test the limits of handling were reached.

VI. Conclusion

This paper presents a new method for estimating lateral tire forces and sideslip angle, that is to say two of the most important parameters affecting vehicle stability and the risk of leaving the road. The developed observer is derived from a simplified four-wheel vehicle model and is based on unscented Kalman filtering technique. Tire-road interaction is represented by the Dugoff model.
A comparison with real experimental data demonstrates the potential of the estimation process. It is shown that it may be possible to replace expensive correvit and dynamometric hub sensors by real-time software observers. This is one of the important results of our work. Another important result concerns the estimation of individual lateral forces acting on each tire. This can be seen as an advance with respect to the current vehicle-dynamics literature.
Future studies will improve the vehicle/road model in order to widen validity domains for the observer, and will take into account road irregularities and road bank angle. Moreover, it will be of major importance to study the effect of coupling longitudinal/lateral dynamics on lateral tire behavior.

	Max $\|\|\|$	Mean %	Std %
F_{y11}	2180 (N)	8.23	4.80
F_{y12}	4070 (N)	3.70	3.74
F_{y21}	1441 (N)	7.51	3.52
F_{y22}	2889 (N)	1.91	1.77
β	0.027 (rad)	8.32	6.41

TABLE I
Maximum absolute values, normalized mean errors, and normalized Std.

References

[1] Y. Hsu and J. Chistian Gerdes, *Experimental studies of using steering torque under various road conditions for sideslip and friction estimation*, Proceedings of the 2007 IFAC Symposium on Advances in Automotive Control, Monterey, California.
[2] D. Lechner, *Embedded laboratory for vehicle dynamic measurements*, 9th International symposium on advanced vehicle control, Kobe, Japan, Octobre 2008.
[3] P. Bolzern, F. Cheli, G. Falciola and F. Resta, *Estimation of the nonlinear suspension tyre cornering forces from experimental road test data*, Vehicle System Dynamics, volume 31, pages 23-24, 1999.
[4] G. Baffet A. Charara, D. Lechner and D. Thomas, *Experimental evaluation of observers for tire-road forces, sideslip angle and wheel cornering stiffness*, Vehicle System Dynamics, volume 45, pages 191-216, june 2008.
[5] U. Kiencke and L. Nielsen, *Automotive control systems*, Springer, 2000.
[6] G. Baffet, A. Charara and J. Stephant, *An observer of tire-road forces and friction for active-security vehicle systems*, IEEE/ASME Transactions on Mechatronics, volume 12, issue 6 pages 651-661, 2007.
[7] J. Dugoff, P. Fanches and L. Segel, *An analysis of tire properties and their influence on vehicle dynamic performance*, SAE paper (700377), 1970.
[8] Hans B. Pacejka, *Tyre and vehicle dynamics*, Elsevier, 2002.
[9] J. Dakhlallah, S. Glaser, S. Mammar and Y. Sebsadji*Tire-road forces estimation using extended Kalman filter and sideslip angle evaluation*, American Control Conference, Seatle, Washington, U.S.A, June 2008.
[10] W.F. Milliken and D.L. Milliken, *Race car vehicle dynamics*, Society of Automotive Engineers, Inc, U.S.A, 1995.
[11] M. Doumiati, A. Victorino, A. Charara, D. Lechner and G. Baffet, *An estimation process for vehicle wheel-ground contact normal forces*, IFAC WC'08, Seoul Korea, july 2008.
[12] H. Nijmeijer and A.J. Van der Schaft, *Nonlinear dynamical control systems*, Springer Verlag, 1991.
[13] J. Stéphant, A. Charara and D. Meizel, *Virtual sensor, application to vehicle sideslip angle and transversal forces*, IEEE Transactions on Industrial Electronics. vol.51, no. 2, April 2004.
[14] G. Baffet, *Développement et validation exprimentale d'observateurs des forces de contact pneumatique/chaussée d'une automobile*, Ph.D thesis, University of Technology of Compiègne, France, 2007.
[15] N. K. M'Sirdi, A. Rabhi, N. Zbiri and Y. Delanne, *Vehicle-road interaction modelling for estimation of contact forces*, Vehicle System Dynamics, volume 43, pages 403-411, 2005.
[16] S. J. Julier and J. K. Uhlman, *A new extension of the Kalman filter to nonlinear systems*, International Symposium Aerospace/Defense Sensing, Simulation and Controls, Orlando, USA, 1997.